ESC European Society of Cardiology

Cardiovascular Research (2019) **115**, 1205–1216
doi:10.1093/cvr/cvz040

Mesenchymal stromal cell-derived exosomes attenuate myocardial ischaemia-reperfusion injury through miR-182-regulated macrophage polarization

Jinxuan Zhao[1†], Xueling Li[2†], Jiaxin Hu[1†], Fu Chen[1], Shuaihua Qiao[1], Xuan Sun[1], Ling Gao[1], Jun Xie[1]*, and Biao Xu[1]*

[1]Department of Cardiology, Drum Tower Hospital, Medical School of Nanjing University, No. 321 Zhongshan Road, Nanjing 210008, China; and [2]Department of Cardiology, Zhejiang Provincial People's Hospital, People's Hospital of Hangzhou Medical College, No. 158 Shangtang Road, Hangzhou 310014, China

Received 29 September 2018; revised 13 January 2019; editorial decision 4 February 2019; accepted 7 February 2019; online publish-ahead-of-print 8 February 2019

Time for primary review: 22 days

Aims Mesenchymal stromal cells (MSCs) gradually become attractive candidates for cardiac inflammation modulation, yet understanding of the mechanism remains elusive. Strikingly, recent studies indicated that exosomes secreted by MSCs might be a novel mechanism for the beneficial effect of MSCs transplantation after myocardial infarction. We therefore explored the role of MSC-derived exosomes (MSC-Exo) in the immunomodulation of macrophages after myocardial ischaemia/reperfusion (I/R) and its implications in cardiac injury repair.

Methods and results Exosomes were isolated from the supernatant of MSCs using gradient centrifugation method. Administration of MSC-Exo to mice through intramyocardial injection after myocardial I/R reduced infarct size and alleviated inflammation level in heart and serum. Systemic depletion of macrophages with clodronate liposomes abolished the curative effects of MSC-Exo. MSC-Exo modified the polarization of M1 macrophages to M2 macrophages both *in vivo* and *in vitro*. miRNA sequencing of MSC-Exo and bioinformatics analysis implicated miR-182 as a potent candidate mediator of macrophage polarization and toll-like receptor 4 (TLR4) as a downstream target. Diminishing miR-182 in MSC-Exo partially attenuated its modulation of macrophage polarization. Likewise, knock down of TLR4 also conferred cardioprotective efficacy and reduced inflammation level in a mouse model of myocardial I/R.

Conclusion Our data indicate that MSC-Exo attenuates myocardial I/R injury in mice via shuttling miR-182 that modifies the polarization status of macrophages. This study sheds new light on the application of MSC-Exo as a potential therapeutic tool for myocardial I/R injury.

Keywords Myocardial ischaemia/reperfusion injury • Mesenchymal stromal cells • Exosomes • Macrophage polarization • MicroRNA

This article is part of the Spotlight Issue on Cardioprotection Beyond the Cardiomyocyte.

1. Introduction

Acute myocardial infarction (MI) is a major cause of death and disability worldwide. Timely reperfusion therapy is needed for reducing acute myocardial ischaemic injury and limiting infarct size. However, the process of reperfusion could induce further damage known as myocardial reperfusion injury.[1] The ischaemia/reperfusion (I/R) process triggers an inflammatory cascade in the heart. The intensity and duration of this

* Corresponding authors. Tel: 86-025-68182812; fax: 86-025-68182812, E-mail: darcy_pann@hotmail.com (J.X.); Tel: 86-025-68182812; fax: 86-025-68182812, E-mail: xubiao62@nju.edu.cn (B.X.)

† These authors contributed equally to this article.

inflammatory reaction are intimately associated with myocardial injury and scar formation.[2,3] In this process, macrophages play an important role in the modulation of cardiac inflammation.[4] After reperfusion, M1 macrophages generates a pro-inflammatory environment and removes cell debris. Gradually, M2 macrophages become more prevalent. The M2 macrophages secrete not only anti-inflammatory cytokines but also a mixture of growth factors and play a critical role in wound healing and scar formation. Hence, both the two distinctive phenotypes are important for infarct healing.[5] The shift in balance between M1 and M2 macrophages, contributing to earlier and more M2 macrophage infiltration, might be a potential target for the treatment of myocardial I/R injury.

Mesenchymal stromal cells (MSCs) are a unique stromal cell type that confers functional and structural benefits in ischaemic heart disease, including reduction of infarct size, improvement of cardiac function, enhanced angiogenesis, and modulation of inflammatory response.[6] Several studies have disclosed that MSCs can reduce pro-inflammatory cytokines produced in macrophages, and trigger the macrophage to polarize towards the anti-inflammatory M2 phenotype *in vivo* and *in vitro*.[7,8] Nonetheless, the underlying mechanism is still fragmentary and incomplete. Accumulating evidence indicated that MSC exerted its benefit on myocardium via its paracrine effect rather than differentiated into myocytes.[9] Exosomes are thought to be a potent secretory component of MSCs containing a specific payload of small RNAs and protein, which play an important role in MSC-mediated biological effect.[10] Several recent studies have implicated that MSC-derived exosomes (MSC-Exo) can improve recovery in animal models of tissue injury and inflammatory diseases.[11–14] However, it remains unknown whether MSC-Exo could induce macrophages to create an anti-inflammatory environment under myocardial I/R injury. In this study, we demonstrated the immunomodulatory effect of MSC-Exo on macrophages in myocardial I/R model, which is mainly through passing on exosomal miR-182 in order to inhibit toll-like receptor 4 (TLR4) activity.

2. Methods

2.1 Animal experimental protocol

All procedures with animals were approved by the Institutional Ethics Committee of Nanjing Drum Tower Hospital (Approval No. 20011141) and performed in accordance with the guidelines set forth in the Guide for the Care and Use of Laboratory Animals published by the National Institutes of Health (Eighth Edition). C57BL/6 mice and BALB/c mice were purchased (8 weeks of age) from the Model Animal Research Center of Nanjing University. TLR4$^{-/-}$ mice on a C57BL/6 background were purchased from Jackson Laboratory (stock number 029015). Age-matched C57BL/6 mice served as controls. Animals were fed a standard laboratory diet with free access to food and water, and kept in a temperature (22 ± 1°) and humidity (65–70%) controlled room, with a 12-h light–dark cycle. After study, all animals were anaesthetized by isoflurane inhalation (1.5–2%) and then euthanized by cervical dislocation.

Myocardial I/R model was established on 8-week male C57BL/6 mice. Mice were anaesthetized by isoflurane inhalation (1.5%-2%) and ventilated with room air using a rodent ventilator. Thoracotomy was performed at the 4th intercostal space to expose the heart and left anterior descending coronary artery (LAD). LAD was ligated with a 7-0 silk suture and was subsequently released after 45 min to allow for reperfusion. Immediately after reperfusion, the peri-infarct myocardial region was injected at three different points with a total of 25 μL of phosphate-buffered saline (PBS) containing 50 μg MSC-Exo. Control mice were injected with 25 μL PBS alone. In the sham-operated group, the LAD was not ligated. For macrophage depletion studies, C57BL/6 mice were intravenously injected with 150 μL (5 mg/mL) clodronate liposomes (Liposoma, The Netherlands) 1 day prior to and 1 day following myocardial I/R injury.

2.2 Exosome isolation and identification

When MSCs reached 70–80% confluency, culture medium was replaced with that containing 5% exosome-depleted foetal bovine serum (System Biosciences, Inc.) and cultured for 48 h. Exosomes were isolated using differential centrifugation based on previously described methods with slight modifications.[15,16]

The morphology of exosomes was observed using transmission electron microscope (JEM-1011 Japan). After isolation, 10 μL exosomes were diluted in 1 mL of filtered PBS and size distribution was measured by NanoSight NS300 (Malvern, UK). Exosomes were then identified by the marker proteins CD9, CD63 TSG101, and Alix using western blotting. The quantity of exosomes was determined by BCA assay (Thermo Scientific) for measurement of total protein. The uptake of DiI-labelled MSC-Exo was determined by confocal microscopy. Detailed descriptions are provided in Supplementary material online.

2.3 Statistical analysis

Data from at least five independent experiments were presented as mean ± SD, unless otherwise indicated. To determine differences between groups at a single time point, data were tested using either two-tailed, unpaired, Student's *t*-test or one-way analysis of variance (ANOVA) followed by Tukey's multiple comparisons test. To determine differences between groups at multiple time points, data were tested using two-way ANOVA followed by Bonferroni's multiple comparisons test. All analyses were performed using Prism 6 software (GraphPad), and only differences with a *P*-value of less than 0.05 were considered statistically significant.

3. Results

3.1 Characterization of MSC-Exo

Mouse bone marrow-derived MSCs isolated from the tibia and femoral marrow compartments presented as long spindle-shaped fibrocyte-like adherent cells and were identified by fluorescence-activated cell sorter analysis as previously described.[17] We purified exosomes from the culture supernatants of MSCs by serial differential centrifugation plus ultracentrifugation. Then the morphology and phenotypes of isolated particles were identified according to the characteristics of exosomes.[15] First, the nanoparticle tracking analysis (NTA) demonstrated that the concentration of the particles and the diameters of the particles were within the range of 50–150 nm, with mode of 142 nm (see Supplementary material online, *Figure S1A*). Transmission electron microscopy showed that the isolated MSC vesicles had a cup-shaped canonical exosome morphology with double-layer membrane structure (see Supplementary material online, *Figure S1B*). Further, western blot analysis confirmed that the particles expressed CD63, CD9, TSG101, and Alix, which are widely recognized molecular markers for exosomes (see Supplementary material online, *Figure S1C*). Therefore, the above properties indicated that MSC-derived particles collected in our experiments were exosomes. For exosomes quantification, the correlation of BCA and NTA quantification methods were evaluated. We found that protein weight in these particle fractions measured by BCA assay was strongly correlated with particle number measured by NTA (see Supplementary

material online, *Figure S1D*). Thus, the quantity of exosomes was determined by BCA assay for subsequent study.

3.2 MSC-Exo administered following reperfusion reduced infarct size and inflammation in a mouse model

To investigate the role of MSC-Exo in myocardial I/R injury, we subjected mice to 45 min of ischaemia followed by reperfusion. Exosomes (or vehicle) were then delivered to myocardium immediately after reperfusion. The dose of exosomes was determined according to our preliminary dose ranging experiment (see Supplementary material online, *Figure S2*) and previous published studies.[14,18] After treatment with MSC-Exo, cardiac function was better preserved (*Figure 1A* and *B*) and infarct size (IS/AAR) was reduced relative to vehicle (PBS) control 3 days post–operation (*Figure 1C* and *D*). Three weeks after myocardial I/R injury, MSC-Exo still improved cardiac function (*Figure 1A* and *B*), preserved left ventricular systolic and diastolic dimensions (see Supplementary material online, *Figure S3A*), attenuated fibrosis (see Supplementary material online, *Figure S3B* and *C*), and reduced hypertrophy of cardiomyocytes relative to vehicle control (see Supplementary material online, *Figure S3D*). No changes in vessel density were observed 3 weeks after myocardial I/R (see Supplementary material online, *Figure S3E*). Thus, MSC-Exo administered immediately after myocardial I/R was able to reduce myocardial injury, leading to sustained functional and structural benefits.

From the histological assessment of heart tissues 3 days after myocardial I/R, we found reduced inflammatory cell infiltration in MSC-Exo-treated mice (*Figure 1E*), indicating that MSC-Exo could modulate inflammation following myocardial I/R. Delivery of MSC-Exo to the heart reduced neutrophil ($Ly6g^+$) infiltration within the heart. While, T cells, such as cytotoxic T cells ($CD8^+$) and helper T cells ($CD4^+$), were unaltered (see Supplementary material online, *Figure S4*). We also measured the concentrations of pro-inflammatory cytokine IL-6 and anti-inflammatory cytokine IL-10 in the serum and heart tissues. Either 3 days or 1 week after the myocardial I/R operation, the levels of these cytokines were all elevated in heart tissues of I/R injured mice as compared with the sham-operated mice. There was a more significant reduction in the concentrations of IL-6 in the heart tissues of MSC-Exo-treated mice vs. the PBS-treated mice (*Figure 1F*). Conversely, the concentration of IL-10 was significantly increased in the MSC-Exo-treated mice compared with that in PBS-treated animals (*Figure 1G*). The similar altered patterns were also shown in the serum levels of IL-6 and IL-10 (*Figure 1H* and *I*). These data suggested that MSC-Exo alleviated cardiac inflammation following myocardial I/R injury.

3.3 Systemic depletion of macrophages using clodronate liposomes reduced the efficacy of MSC-Exo therapy

Since previous studies demonstrated that macrophages played a critical role in the modulation of cardiac inflammation after myocardial I/R injury,[4,19] we investigated the role of macrophages in the benefits of MSC-Exo therapy. To do so, we administered clodronate [dichloromethylene diphosphonate (Cl_2MDP)] liposomes 24 h prior to and following myocardial I/R, MSC-Exo (or vehicle) were delivered to myocardium immediately after reperfusion (*Figure 2A*). As expected, clodronate significantly reduced blood, spleen, and cardiac macrophage populations using flow cytometry analysis (*Figure 2B* and *C*). Clodronate itself did not aggravate I/R injury, as we observed no significant difference in infarct size and cardiac function between the PBS-treated group and the PBS and Cl_2MDP-treated group. However, clodronate attenuated the benefits of MSC-Exo, that is, infarct size was increased in the group treated with MSC-Exo and Cl_2MDP relative to that in the MSC-Exo-treated group 3 days post the I/R operation (*Figure 2D* and *E*). Mice treated with MSC-Exo had improved values of ejection fraction (EF %) and fractional shortening (FS %), compared with the MSC-Exo and Cl_2MDP group (*Figure 2F*). Collectively, our results suggested that depletion of macrophages impaired the benefits of MSC-Exo, indicating that macrophages were required for the cardioprotective effects of MSC-Exo therapy. The effects of MSC-Exo largely relied on its interactions with macrophages. Thus, we went on to investigate, in detail, the potential effects of MSC-Exo on macrophage quantity and subpopulation.

3.4 MSC-Exo reduced the number of M1 macrophages and promoted macrophages transforming towards M2-like phenotype under myocardial I/R injury

To investigate the potential effects of MSC-Exo on macrophage, we first examined the quantity of macrophages within heart under MSC-Exo treatment. We collected the left ventricle tissues near apex of hearts 3 days after operation and observed that the proportion of $CD11b^+F4/80^+$ macrophages was significantly increased in the heart tissue of the PBS-treated myocardial I/R mice compared with that of the sham-operated group. Whereas the administration of MSC-Exo did not alter total macrophage population when compared with PBS-treated mice (*Figure 3A* and *B*). These results indicated that MSC-Exo did not affect the quantity of macrophages accumulated in injured heart.

It is well recognized that macrophages exhibit the capacity to switch between M1 and M2 under injury. We therefore asked whether MSC-Exo could polarize macrophages towards the M1 or M2 phenotype under myocardial I/R. The populations of M1 and M2 phenotypes were measured using flow cytometry analysis. Interestingly, the M1 macrophages ($iNOS^+CD206^-$) were remarkably reduced in the MSC-Exo-treated mice compared with the PBS-treated mice. Meanwhile, the M2 macrophages ($iNOS^-CD206^+$) were increased by MSC-Exo treatment (*Figure 3A* and *B*). Furthermore, the quantitative real–time PCR (qRT-PCR) analysis for M1 and M2 gene expression also showed that M1 markers (iNOS, IL-1β, IL-6, and TNFα) were significantly reduced, whereas the M2 markers were increased, such as Arg1, IL-10, CD206, and TGFβ (*Figure 3C* and *D*), which was consistent with western blot analysis (*Figure 3E* and *F*). Collectively, these data demonstrated that MSC-Exo polarized macrophages away from the M1 phenotype and towards an M2-like state under myocardial I/R injury.

3.5 MSC-Exo converted inflammatory macrophages to M2 phenotype *in vitro*

To better understand how MSC-Exo interacts with macrophages, MSC-Exo was added to the cultured RAW264.7 cells. The DiI (red)-labelled MSC-Exo was internalized into macrophages and localized in the cytoplasm within 6 h (*Figure 4A*). To further validate the direct effects of MSC-Exo on macrophages, lipopolysaccharide (LPS) was added to culture systems prior to the addition of MSC-Exo in order to induce an inflammatory micro-environment. Six hours later, MSC-Exo or PBS was added to the stimulated macrophages. About 48 h later, we detected the concentrations of IL-6 and IL-10 in the culture supernatants and the expression levels of iNOS and Arg1. We found that the MSC-Exo inhibited the LPS-induced IL-6 and iNOS production and promoted the up-regulation of IL-10 and Arg1 (*Figure 4B–D*). Furthermore, flow cytometry

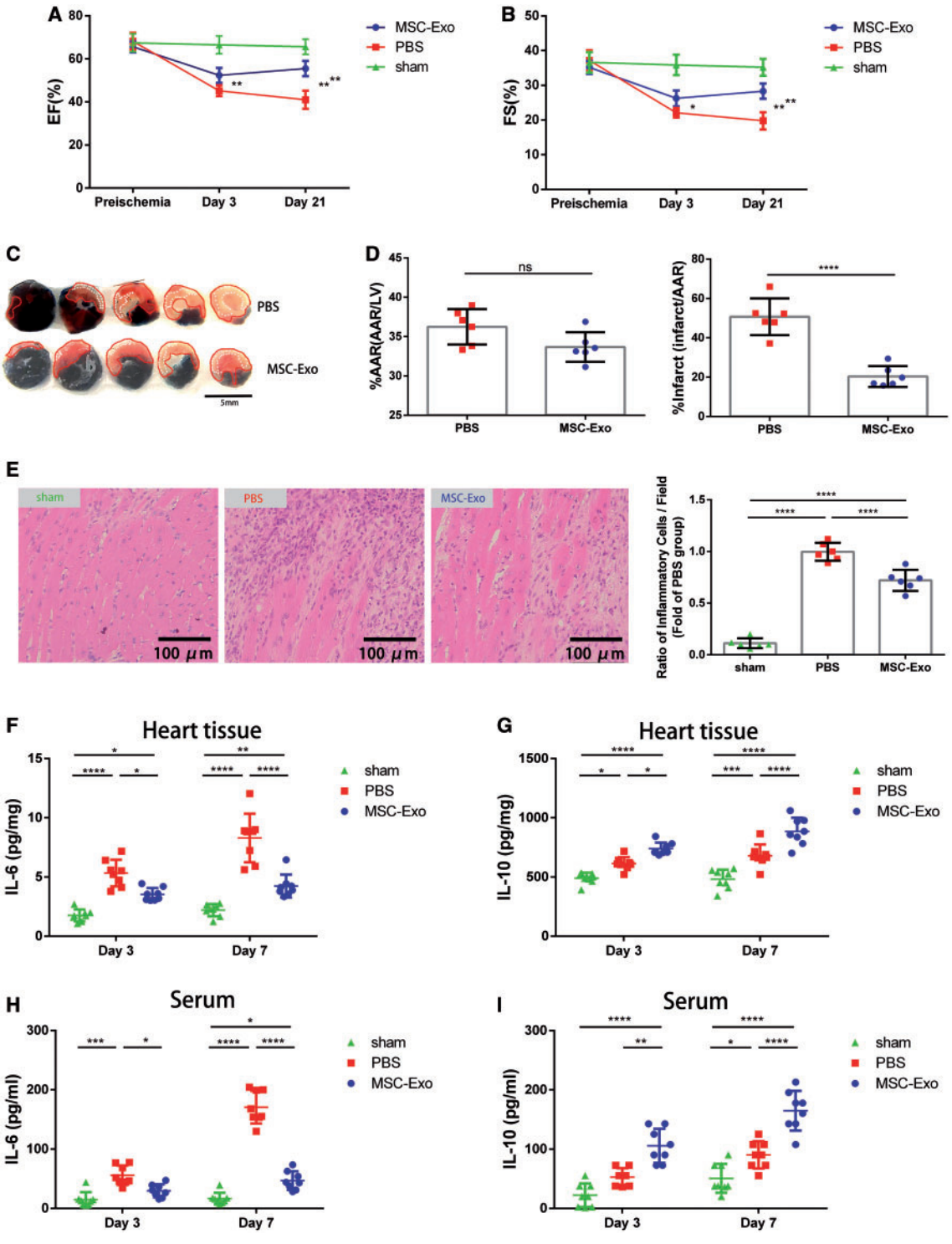

Figure 1 Intramyocardial infusion of MSC-Exo attenuates myocardial I/R injury and alleviates cardiac inflammation in mice. EF% (*A*) and FS% (*B*) of sham-operated, PBS–treated, and MSC-Exo-treated mice measured by echocardiography 3 days and 3 weeks following myocardial I/R injury (sham, $n = 5$; PBS, $n = 8$; MSC-Exo, $n = 8$). (*C*) Representative images of Evans Blue and TTC-stained hearts isolated from mice 3 days following treatment with PBS or MSC-Exo. Area-at-risk (AAR; red line) and infarct size (IS; white dotted line). Scale bar = 5mm. (*D*) Quantitative analysis of the percentage AAR and percentage infarct of hearts in (*C*) ($n = 6$). (*E*) HE staining and quantification of inflammatory cell infiltration (%) within the ischaemic heart 3 days following operation ($n = 6$). Scale bar = 100 μm. Cytokine expression of IL-6 (*F*) and IL-10 (*G*) in the hearts of mice treated with PBS or MSC-Exo 3 days and 7 days after myocardial I/R ($n = 8$). Concentration of cytokines IL-6 (*H*) and IL-10 (*I*) in serum 3 days and 7 days after I/R ($n = 8$). Graphs depict mean ± SD. Statistical significance was determined using Student's *t*-test for two group's comparison, one-way ANOVA followed by Tukey's multiple comparisons test for multiple group comparisons and two-way ANOVA followed by Bonferroni's multiple comparisons test for comparison between different groups over time. $^{*}P < 0.05$; $^{**}P < 0.01$; $^{***}P < 0.001$; $^{****}P < 0.0001$; ns, not significant.

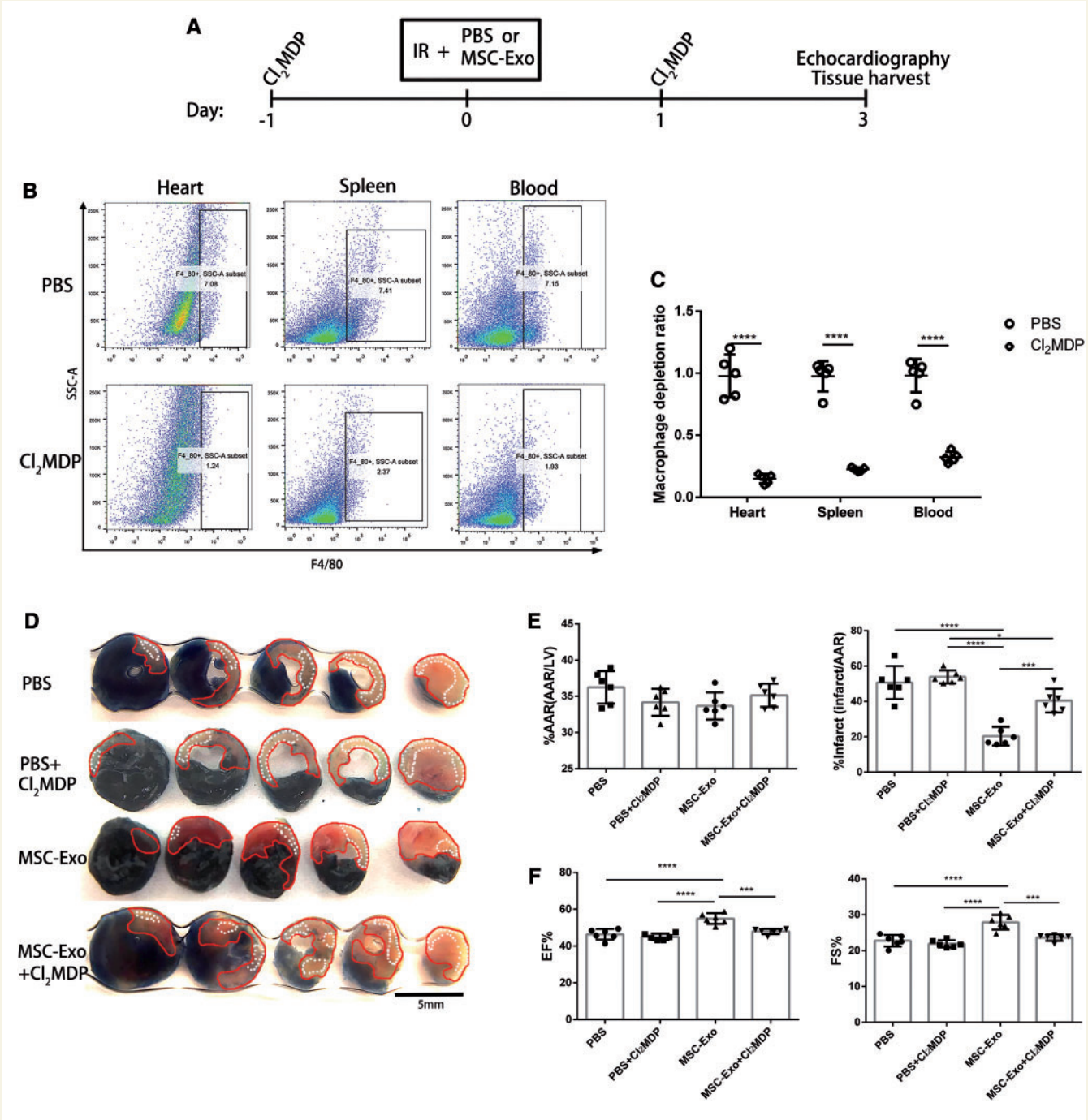

Figure 2 Systemic depletion of endogenous macrophages reduces the efficacy of MSC-Exo therapy. (*A*) Schematic of macrophage depletion protocol using Cl_2MDP liposomes. (*B*) Representative flow cytometry plots of macrophage population in the spleens, blood, and hearts from Cl_2MDP- and PBS-treated animals 3 days after I/R. (*C*) Pooled flow cytometry data from (*B*) ($n = 5$). (*D*) Representative images of Evans Blue and TTC-stained hearts from mice sacrificed 3 days after infusion of MSC-Exo or vehicle with or without macrophage depletion prior to myocardial I/R injury. Area-at-risk (AAR; red line) and infarct size (IS; white dotted line). Scale bar = 5 mm. (*E*) Quantification of percentage AAR and percentage infarct in hearts from groups defined in (*D*) ($n = 6$). (*F*) EF% and FS% measured by echocardiography 3 days following myocardial I/R injury ($n = 6$). Graphs depict mean ± SD. Statistical significance was determined using Student's *t*-test and one-way ANOVA followed by Tukey's multiple comparisons test. $^{*}P < 0.05$; $^{***}P < 0.001$; $^{****}P < 0.0001$.

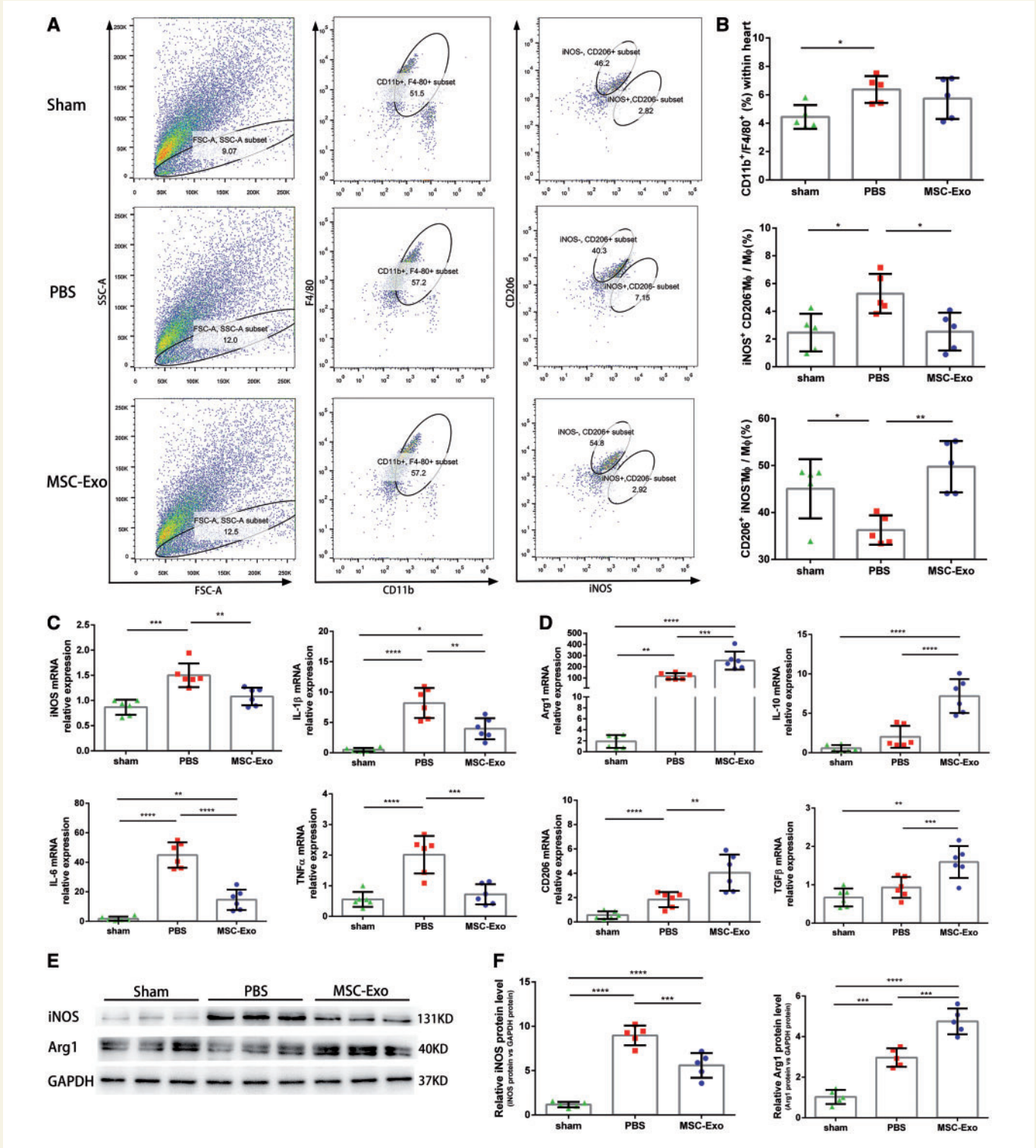

Figure 3 Effects of MSC-Exo on macrophage infiltration and polarization following myocardial I/R. (*A*) Representative flow cytometry plots showing the gating strategy used to determine total macrophage in heart ($CD11b^+F4/80^+$), M1 phenotype($CD11b^+F4/80^+iNOS^+CD206^-$) and M2 phenotype ($CD11b^+F4/80^+iNOS^-CD206^+$). (*B*) Quantification of total macrophages, M1 macrophages and M2 macrophages within heart tissues 3 days following treatment with PBS or MSC-Exo ($n = 5$). (*C*) Gene expression profiles of pro-inflammatory cytokines and M1 macrophage marker in the hearts of mice sacrificed 3 days after myocardial I/R ($n = 6$). (*D*) Gene expression profiles of anti-inflammatory cytokines and M2 macrophage marker in the hearts of mice treated with PBS or MSC-Exo 3 days after myocardial I/R ($n = 6$). Expression of interest genes is normalized to GADPH and given as a relative change. (*E*) Representative images of western blot to assess levels of iNOS and Arg1 in the hearts of mice treated with PBS or MSC-Exo 3 days after I/R ($n = 5$). (*F*) Quantification of band intensities in (*E*). All data are mean ± SD. Statistical significance was determined using one-way ANOVA followed by Tukey's multiple comparisons test. $^*P < 0.05$; $^{**}P < 0.01$; $^{***}P < 0.001$; $^{****}P < 0.0001$.

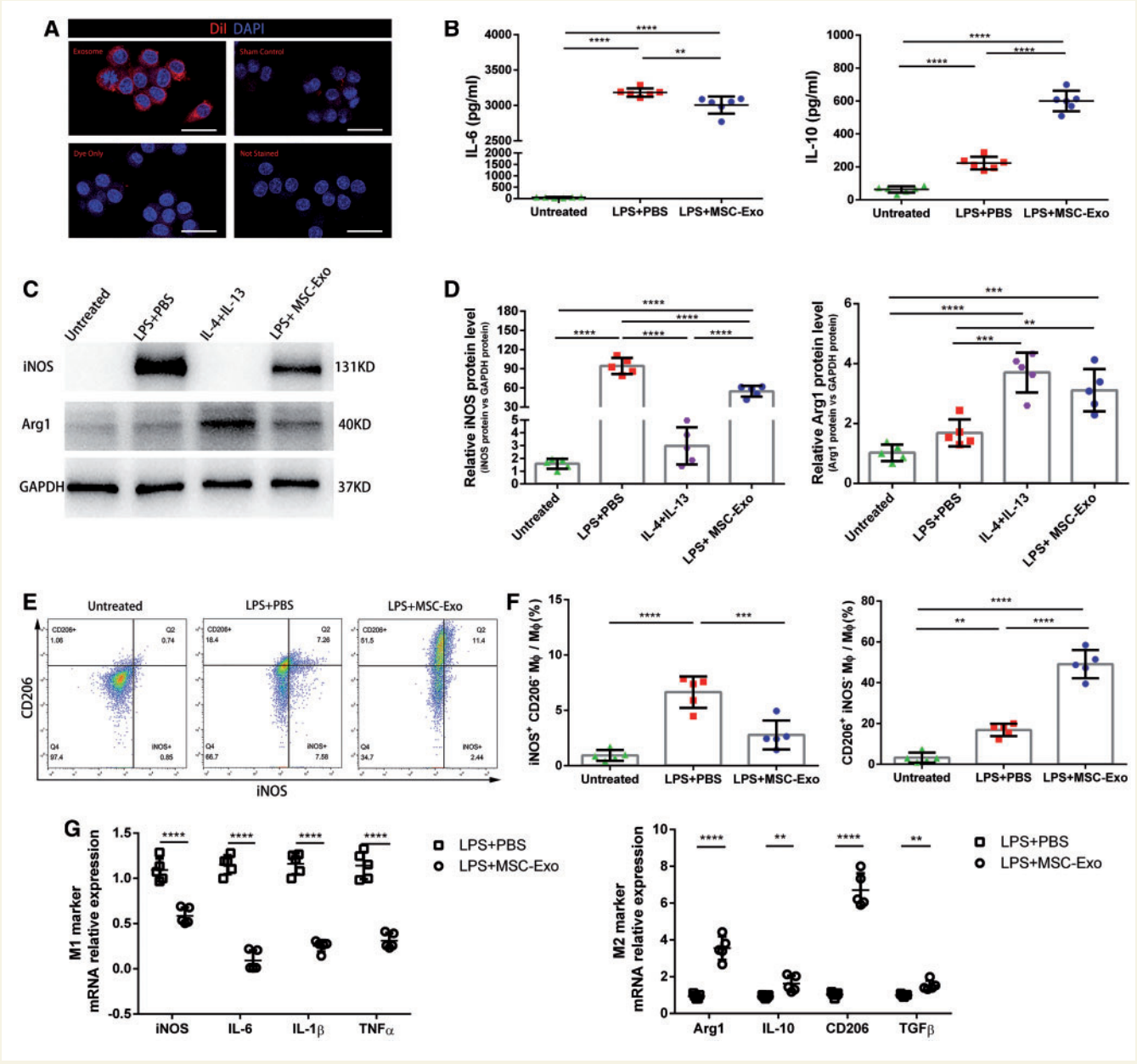

Figure 4 MSC-Exo facilitates the polarization of macrophages to M2 phenotype under inflammatory environment. (*A*) Representative images of the uptake of Dil-labelled exosomes (red) by RAW264.7 cells (DAPI blue) and fluorescence uptake with sham control and dye-only samples. Sham control, aliquots isolated from equal volume of MSC culture medium containing 5% exosome-free FBS in the absence of cells stained with Dil; Dye-only, PBS negative control stained with the Dil; Non-stained, background RAW264.7 cells fluorescence without addition of a sample. Scale bar = 25 μm. (*B*) Concentration of cytokine IL-6 and IL-10 in supernatants of LPS-stimulated RAW 264.7 cells after culturing with MSC-Exo or PBS for 48 h ($n = 6$). (*C*) Western blot assay for iNOS and Arg1 expression in LPS-stimulated RAW 264.7 cells after culturing with MSC-Exo or PBS for 48 h. (*D*) Quantitative analysis of iNOS, Arg1 levels in (*C*) ($n = 5$). (*E*) Representative flow cytometry plots showing the percentages of M1 ($iNOS^+CD206^-$) and M2 ($iNOS^-CD206^+$) phenotype in LPS-stimulated peritoneal macrophages after culturing with MSC-Exo or PBS for 48 h. (*F*) Quantification of flow cytometry data in (*E*) ($n = 5$). (*G*) Gene expression profiles of M1 markers (iNOS, IL-1β, IL-6, and TNFα) and M2 markers (Arg1, IL-10, CD206, and TGFβ) in LPS-stimulated peritoneal macrophages after culturing with MSC-Exo or PBS for 48 h ($n = 5$). Expression of interest genes is normalized to GADPH and given as relative change. Data are presented as mean ± SD. Statistical analysis was performed with Student's *t*-test and one-way ANOVA followed by Tukey's multiple comparisons test. $^{**}P < 0.01$; $^{***}P < 0.001$; $^{****}P < 0.0001$.

analysis showed that the ratio of M2 macrophages was significantly increased and that of M1 macrophages was markedly reduced in the MSC-Exo group (see Supplementary material online, *Figure S5B* and *C*). Same trends were observed when MSC-Exo interacted with peritoneal macrophages (*Figure 4E* and *F*). The qRT–PCR results also showed that after MSC-Exo treatment, peritoneal macrophages dramatically produced more anti-inflammatory cytokines (IL-10, TGFβ) and less pro-inflammatory cytokines, including IL-1β, IL-6, and TNFα (*Figure 4G*). Taken together, these data indicated that MSC-Exo facilitated the polarization of macrophages to M2 rather than M1.

3.6 miR-182 was candidate effector of MSC-Exo mediated macrophage polarization

Studies suggested that exosomes had an intriguing role on cellular communication through the exchange of miRNAs or proteins between cells.[18,20] Therefore, we determined to investigate whether MSC-Exo contained any pivotal miRNAs that contributed to its immunomodulatory effect. To understand how MSC-Exo regulates macrophage polarization, we performed small RNA sequencing on MSC-Exo and then aligned them to a public available database of exosomal miRNA profiles (ExoCarta). Based on the miRNA profiling in MSC-Exo, we searched for miRNAs reported either involved in inflammation modulation (miR-181, miR-223, miR-124, miR-146a, miR-182, miR-125a),[18,21–23] or cardiac repair (miR-103, miR-221, miR-133, miR-150, miR-21, miR-22, miR-182, miR-125a),[24,25] or enriched in MSC-Exo (miR-21, miR-22, miR-378, miR-182, miR125a, miR-199)[26] as shown in *Figure 5A*. miR-182 and miR-125a stood out as candidates enriched in MSC-Exo probably responsible for macrophage polarization. qRT–PCR further confirmed that miR-182 and miR125a were more abundant in MSC-Exos compared with macrophage-derived exosomes (*Figure 5B*).

Subsequently, we investigated the direct effects of miR-182 and miR-125a on macrophages. We first confirmed that RAW264.7 cells expressed higher levels of miR-182 and miR-125a after transfected with correspondent miRNA mimic (see Supplementary material online, *Figure S6*). To detect the effects of miR-182 and miR-125a on macrophage polarization, the levels of M1 and M2 markers were detected by flow cytometry and qRT–PCR analysis. The results showed that miR-182 mimic obviously facilitated the polarization of macrophages from M1 to M2 under inflammatory environment (*Figure 5C* and *D*; see Supplementary material online, *Figure S7*), whereas miR-125a did not affect the alteration of macrophage phenotypes (see Supplementary material online, *Figure S8*). These results demonstrated that miR-182 might be the key regulatory cargo contained in MSC-Exo accounting for the regulation of macrophage polarization.

To confirm the role of miR-182 in MSC-Exo, we inhibited the function of miR-182 in MSC-Exo by transfecting MSCs with miR-182 inhibitor and subsequently isolated the exosomes (called miR-182 inhibitor MSC-Exo) from the culture supernatants. The FAM-labelled miR-182 inhibitor, which was contained in DiI-labelled exosomes, was internalized into macrophages, as visualized by confocal microscopy (*Figure 5E* and *F*). qRT–PCR analysis demonstrated that the level of miR-182 was significantly reduced in miR-182 inhibitor MSC-Exo compared with negative control (NC) inhibitor MSC-Exo (*Figure 5G*). We then treated LPS-stimulated macrophages with NC inhibitor MSC-Exo or miR-182 inhibitor MSC-Exo for 48 h and then collected the cells for flow cytometry and qRT–PCR analysis. Results showed that the down-regulation of M1 markers (iNOS, IL-1β, IL-6, and TNFα) as well as the up-regulation of M2 markers (CD206, IL-10, Arg1, and TGFβ) induced by NC inhibitor MSC-Exo were partially negated by miR-182 inhibitor MSC-Exo (*Figure 5H* and *I*; see Supplementary material online, *Figure S9*). Thus, miR-182 recapitulated the immunomodulatory effects of MSC-Exo, while inhibiting miR-182 blunted those effects. miR-182 was involved in the MSC-Exo mediated macrophage polarization.

3.7 miR-182 shuttling by MSC-Exo modulated macrophage phenotype through targeting TLR4

To better understand how miR-182 modulates macrophage phenotypes, we focused on the target gene of miR-182 within macrophages. According to the database of miRNA targets (see Supplementary material online, *Figure S10A*), we found that TLR4 might be the potential target relative to inflammation attenuation. To confirm whether TLR4 is a target of miR-182 in macrophage, the expression levels of TLR4 in miR-182 mimic transfected macrophages were measured by qRT–PCR and western blotting. The protein levels of TLR4 were significantly reduced in macrophages transfected with miR-182 mimic, whereas no difference was detected in transcription level (*Figure 6A* and *B*). These results suggested that miR-182 inhibited the expression of TLR4 within macrophages via a post-transcriptional regulation.

Previous findings suggested that there was a reciprocal regulation between the TLR4/NF-κB and PI3K/Akt signalling pathways during myocardial I/R injury.[27,28] Inhibition of TLR4-mediated signalling might increase activation of the PI3K/Akt signalling pathway, which was important for an anti-inflammatory M2 macrophage conversion.[29] Thus, we investigated the crosstalk between TLR4/NF-κB and PI3K/Akt signalling pathways after transfection of macrophages with miR-182. Western blotting analysis revealed that the levels of iNOS, TLR4, and NF-κB p-P65 were significantly down-regulated. Meanwhile, the expression levels of Arg-1, p-PI3K, and p-AKT were markedly up-regulated after transfection with miR-182 mimic (*Figure 6C*; see Supplementary material online, *Figure S10B*).

Subsequently, we investigated the effects of MSC-Exo on TLR4 and its downstream signalling pathways. *In vitro* experiment, we found that the levels of TLR4, MyD88, and NF-κB p-P65 were significantly down-regulated, while the expression levels of p-PI3K and p-AKT were up-regulated after NC inhibitor MSC-Exo treatment. Furthermore, the inhibition of TLR4 and activation of PI3K/Akt were partially reversed when treated with miR-182 inhibitor MSC-Exo (*Figure 6D*; see Supplementary material online, *Figure S10C*). *In vivo*, we also observed significantly decreased levels of TLR4 within myocardium in MSC-Exo-treated mice when compared with PBS-treated mice (*Figure 6E*). These data suggested that miR-182 was involved in the MSC-Exo mediated macrophage polarization by targeting the TLR4/NF-κB/PI3K/Akt signalling cascades.

Several studies have shown that the inhibition of TLR4 is beneficial for alleviating inflammatory responses and lessening additional damage to the already injured myocardium.[30,31] Therefore, we established a myocardial I/R model in TLR4-deficiency mice and wild-type (WT) mice. Three days after myocardial I/R induction, TLR4-deficiency mice showed improved cardiac function (*Figure 6F*), reduced inflammatory cell infiltration and less inflammatory cytokine expression compared with WT mice (see Supplementary material online, *Figure S11A–C*). We further detected the macrophage phenotype in cardiac tissue of TLR4-deficiency and WT mice after myocardial I/R induction. Flow cytometry analysis showed that TLR4 deficiency mice exhibited significantly higher ratio of M2 macrophages and lower ratio of M1 macrophages compared with WT mice, mimicking the effects of MSC-Exo (*Figure 6G* and *H*). These data indicated that inhibition of TLR4 recapitulated the benefits of MSC-Exo *in vivo*. TLR4 inhibition by exosomal miR-182-5p underlied the cardioprotection and immunomodulatory effects of MSC-Exo.

4. Discussion

In this study, we firstly demonstrated the curative effects of MSC-Exo in myocardium healing after myocardial I/R injury. Then we applied the

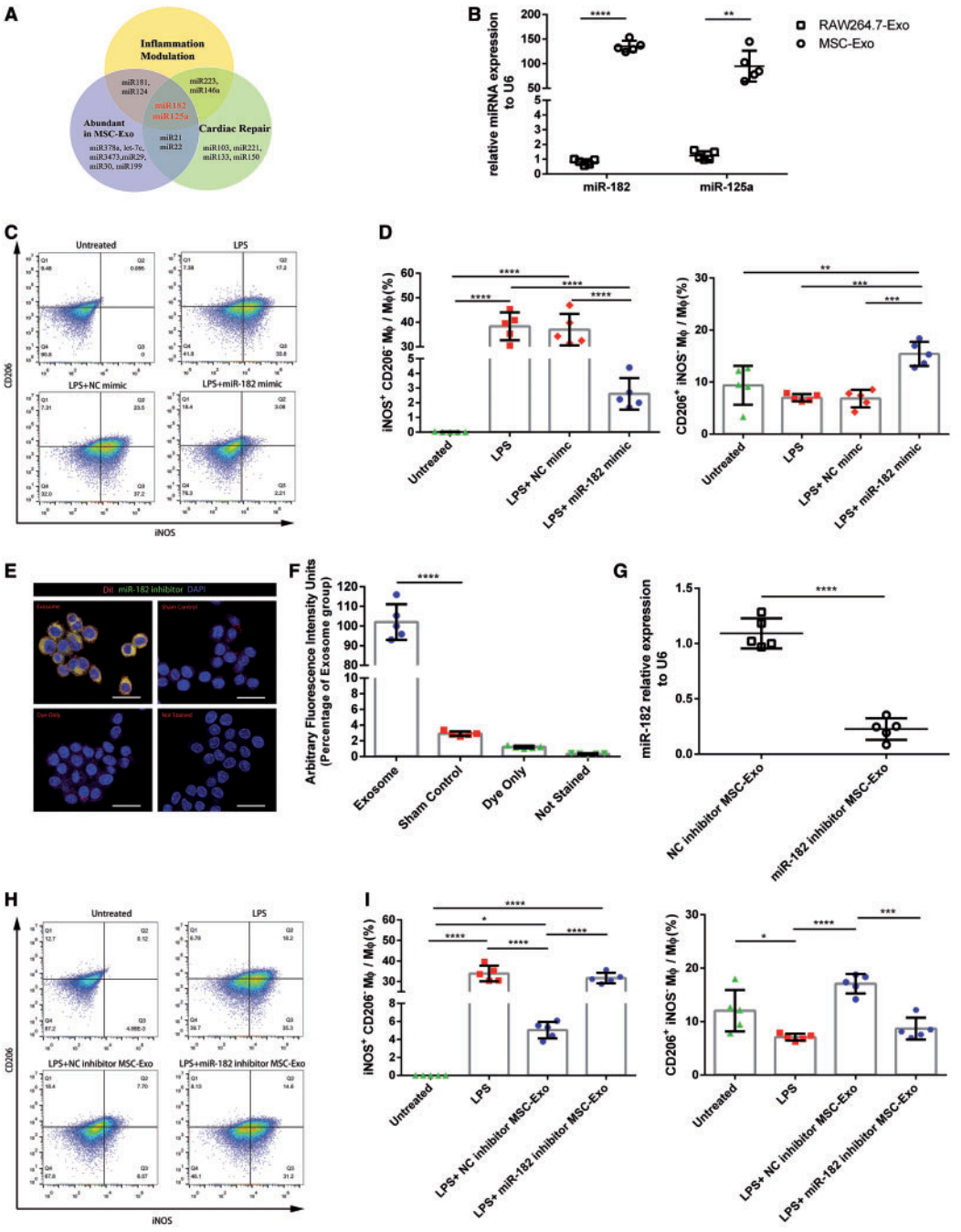

Figure 5 miR-182 is involved in MSC-Exo mediated macrophage polarization *in vitro*. (*A*) Main reported miRNAs participated in inflammation modulation, cardiac repair, and miRNAs abundant in MSC-Exo according to miRNA-sequencing analysis. miR-182 and miR-125a are multifunctional in both fields. (*B*) Real-time PCR analysis of miR-182 and miR-125a levels in exosomes derived from MSCs and RAW264.7 cells ($n = 5$). The expression levels of the miRNAs were normalized to U6. (*C*) Representative flow cytometry plots showing the percentages of M1 ($iNOS^+CD206^-$) and M2 ($iNOS^-CD206^+$) phenotype in LPS-stimulated RAW264.7 cells after transfection with miR-182 mimic or NC mimic for 48 h. (*D*) Pooled flow cytometry data from (*C*) ($n = 5$). (*E*) Representative images of the uptake of miR-182 inhibitor transfected (green) Dil-labelled MSC-Exo (red) by RAW264.7 cells (DAPI blue) and fluorescence uptake with sham control and dye-only samples. Sham control, aliquots isolated from equal volume of MSC culture medium containing 5% exosome-free FBS in the absence of cells stained with Dil; Dye-only, PBS negative control stained with the Dil; Non-stained, background RAW264.7 cells fluorescence without addition of a sample. Scale bar = 25 μm. (*F*) Quantification of arbitrary fluorescence intensity from five different fields of each sample in (*E*) at 400× magnification obtained in a single experiment ($n = 5$). (*G*) Real-time PCR analysis of miR-182 levels in exosomes derived from NC inhibitor MSC-Exo and miR-182 inhibitor MSC-Exo ($n = 5$). (*H*) Representative flow cytometry plots showing the percentages of M1 ($iNOS^+CD206^-$) and M2 ($iNOS^-CD206^+$) phenotype in LPS-stimulated RAW264.7 cells treated with miR-182 inhibitor MSC-Exo or NC inhibitor MSC-Exo for 48 h. (*I*) Quantification of flow cytometry data in (*H*) ($n = 5$). Data are presented as the mean ± SD. Statistical significance was determined using Student's *t*-test and one-way ANOVA followed by Tukey's multiple comparisons test. $^*P < 0.05$; $^{**}P < 0.01$; $^{***}P < 0.001$; $^{****}P < 0.0001$.

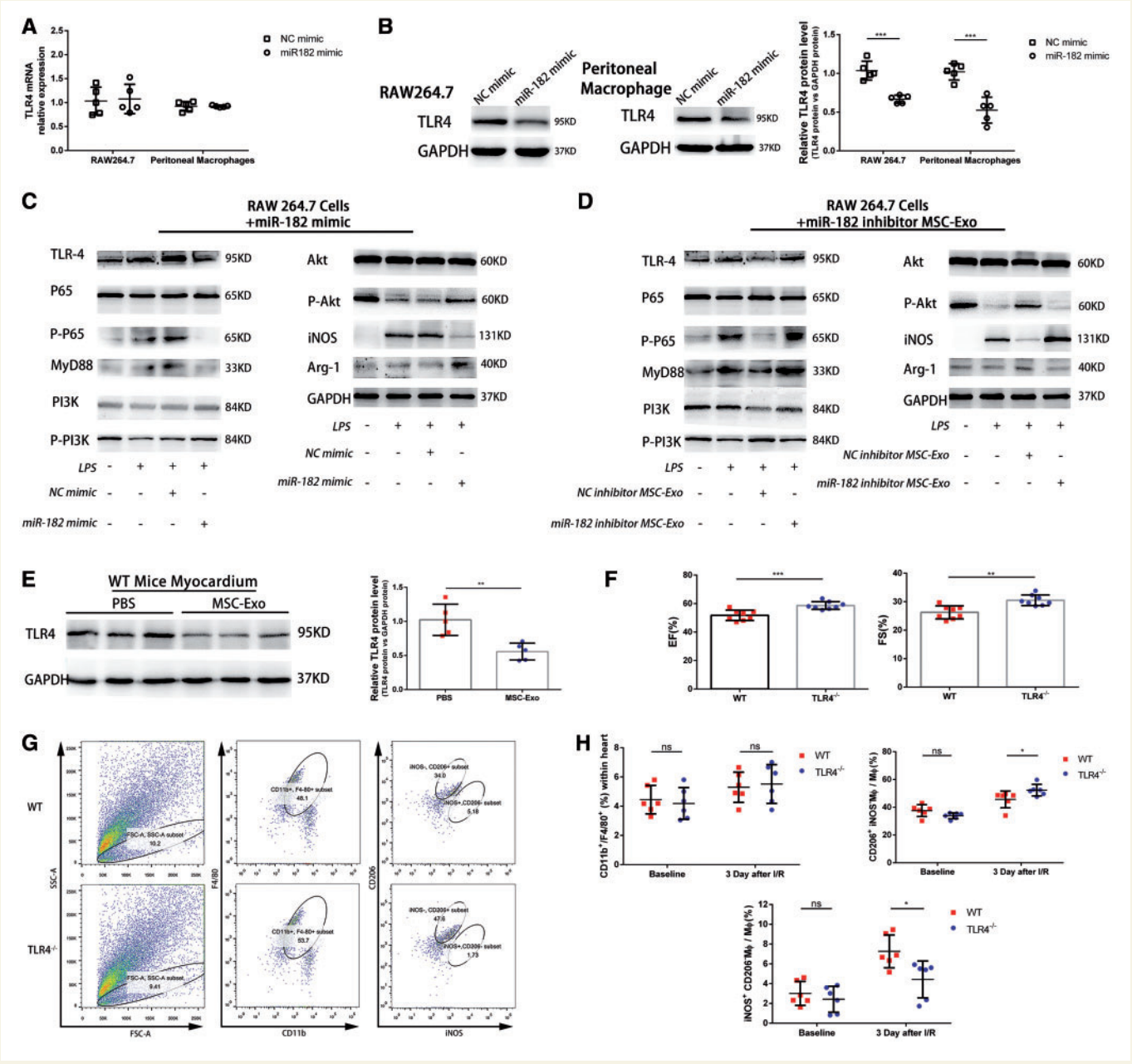

Figure 6 miR-182-5p shuttling by MSC-Exo modulates macrophage phenotype through targeting TLR4. (*A*) TLR4 mRNA relative expression detected by qRT–PCR after transfection of miR-182 mimic or scramble control ($n = 5$). (*B*) Protein levels of TLR4 detected by western blotting after transfection of miR-182 mimic or scramble control ($n = 5$). (*C*) Representative images of western blots for TLR4 and downstream MyD88/NF-κB and PI3K/Akt signalling pathways in LPS-stimulated RAW264.7 cells after transfection with miR-182 mimic or NC mimic for 48 h ($n = 5$). (*D*) Representative images of western blots for TLR4 and downstream MyD88/NF-κB and PI3K/Akt signalling pathways in LPS-stimulated RAW264.7 cells treated with miR-182 inhibitor MSC-Exo or NC inhibitor MSC-Exo for 48 h ($n = 5$). (*E*) Protein levels of TLR4 in cardiac tissue of mice treated with PBS or MSC-Exo 3 days after myocardial I/R ($n = 5$). (*F*) EF% and FS% of TLR4-deficiency mice and WT mice 3 days following myocardial I/R injury ($n = 8$). (*G*) Representative flow cytometry plots showing the percentages of total macrophage ($CD11b^+F4/80^+$), M1 ($CD11b^+F4/80^+iNOS^+CD206^-$) and M2 ($CD11b^+F4/80^+iNOS^-CD206^+$) phenotype within the heart tissue of TLR4-deficiency mice and WT mice 3 days following I/R injury. (*H*) Quantification of total macrophages, M1 macrophages and M2 macrophages within the heart tissue of TLR4-deficiency mice and WT mice in baseline and 3 days following myocardial I/R injury ($n = 6$). Graphs depict mean ± SD. Statistical significance was determined using Student's *t*-test and one-way ANOVA followed by Tukey's multiple comparisons test. $^*P < 0.05$; $^{**}P < 0.01$; $^{***}P < 0.001$; ns, not significant.

macrophage depletion model to reveal that macrophage was mainly downstream target of MSC-Exo. Our work further confirmed that MSC-Exo effectively shifted polarization of macrophages favourable to M2 other than M1 phenotype, which might mitigate inflammatory cascades and enhance subsequent reparative activities, thereby limiting infarct size. Furthermore, we demonstrated that miR-182 was abundant in MSC-Exo, and regulated macrophage phenotype via TLR4/NF-κB pathway.

Following myocardial I/R, a variety of damage-associated molecules are released from necrotic cardiac resident cells, thus induce an inflammatory cascade within the heart.[1] The initial pro-inflammatory response starts with clearance of dead cells and debris, and is gradually replaced by an anti-inflammatory reparative phase, which allows wound healing, and scar formation. The infiltration of inflammatory cells and accumulation of pro-inflammatory cytokines not only clear cellular debris but also give rise to further damage and stress on the surviving cardiomyocytes.[3] Therefore, for over 30 years, a variety of remedies for suppressing this immune reaction has been investigated. However, application of traditional anti-inflammatory drugs to suppress this immune reaction failed to attenuate the injury,[32] which indicated that an effective therapy should not only reduce the length and damage of the inflammatory response but also promote the activation of reparatory pathways. Over the past decade, the immunomodulatory potential of MSCs has generated hope for treatment of many immune-related diseases.[33] MSCs have been found to interact with all cells of the immune system and gently steer the immune reaction towards an anti-inflammatory response. In animal model or human being with MI, MSC transplantations have been found to confer beneficial effect on cardiac repair.[34] However, the detailed mechanism was not fully elucidated. Therefore, whether MSC or its production exerts immunomodulatory effect on myocardial I/R injury need to be identified directly.

Recent studies have demonstrated that interaction between MSCs and the inflammatory niche may largely rely on cell–cell communication through secretion of immunomodulatory secretomes.[35,36] Aside from numerous growth factors and cytokines produced by MSCs, exosomes have gained interest as intriguing paracrine signals that can shuttle payloads from cell to cell.[9] Exosomes are small vesicles secreted by a large variety of cells, which play an important role in these paracrine effects. Several recent reports have demonstrated that several kinds of stem cell-derived exosomes are able to improve global heart function and attenuate ventricular remodelling via inhibiting stress-induced apoptosis, reducing oxidative stress, and stimulating angiogenesis under myocardial ischaemia injury.[14,25,37] However, the possible effect of MSC-Exo on post-myocardial I/R inflammation has been rarely studied. In our study, we firmly demonstrated that the curative effects of MSC-Exo had a strong relation with its modulation of inflammation and lasted along the acute inflammation phase and healing phase.

Macrophages are central mediators of cardiac inflammation, contributing to both the initiation and resolution of inflammation. Several studies have highlighted the importance of macrophages in models of myocardial I/R injury.[18,19] In this study, we used the macrophage depletion model and found that the effects of MSC-Exo largely relied on its interactions with macrophages. It is widely accepted that there exists two typical subtype of macrophages: classically activated M1 macrophages and alternatively activated M2 macrophages.[4] Growing evidence has indicated that MSC has the capability to trigger the macrophage to switch towards the anti-inflammatory M2 phenotype.[7,8] Our work further confirmed that MSC-Exo effectively shifted the polarization state of macrophage from M1 towards M2 phenotype not only *in vitro* but also in myocardial I/R mice. The switch of macrophage phenotype by MSC-Exo mitigated pro-inflammatory cascades and enhanced subsequent reparative activities, thereby limiting infarct size.

miRNAs have been implicated as important components of exosomes and largely decide the effects of exosomes on recipient cells. Among the miRNAs found in exosomes derived from stem cell, some have important immunomodulatory properties, such as miR-21,[25] miR-223,[21] miR-146a,[12] and miR-181b.[18] Probing our own sequencing data against public available exosomal miRNA profiles and miRNA target prediction databases, we identified miR-182 as our top candidate. Until now, studies concerning the relationship between miR-182 and I/R injury are limited, the role of miR-182 in the immunomodulatory effects of MSC-Exo remains uninvestigated. Our results first demonstrated that blocking miR-182 in MSC-Exo blunted the immunomodulatory effects of MSC-Exo on macrophages.

Previous study suggested that miR-182 specifically targeted TLR4 and inactivated TLR4/NF-κB pathway.[38] Whether miR-182 and TLR4/NF-κB pathway was involved in MSC-Exo depended macrophage polarization was explored by our group. Our data confirmed that TLR4 was negatively regulated by either MSC-Exo or miR-182 mimic in macrophages. Meanwhile, MSC-Exo could blunt TLR4 expression within myocardium, indicating that TLR4 may be the underlying target of MSC-Exo mediated macrophage polarization. The inhibition of TLR4 and its downstream MyD88/NF-κB signalling pathway by miR-182 has been shown to alleviate inflammation by negatively polarizing M1 macrophages.[38] On the other hand, detailed mechanism about miR-182 depended M2 conversion remains unclear. Hua *et al.*[39] reported that inhibition of TLR4-mediated signalling could increase the activation of PI3K/Akt signalling pathway, which was important for M2 polarization. Therefore, we examined these two signalling pathways and found that PI3K/AKT were activated and TLR4/NF-κB were inhibited after MSC-Exo treatment or miR-182 transfection. The inhibition of TLR4 and activation of PI3K/Akt were partially reversed when miR-182 level was low in exosomes. These data strongly indicated that miR-182 was involved in the MSC-Exo mediated macrophage polarization by targeting the TLR4/NF-κB/PI3K/Akt signalling cascades. However, the underlying mechanism of the crosstalk between TLR4/NF-κB and PI3K/Akt signalling pathways still needs further exploration.

Despite the compelling evidence pinpointing TLR4 as a likely downstream effector, it is clear that exosomes and their miRNAs have protean effects, which may be synergistic. Picking a single candidate may oversimplify the actual biology. Although our data suggest that exosomal miR-182 has a critical role in the immunomodulation and cardioprotection effect of MSC-Exo, we do not rule out the contribution of other exosomal cargoes. Many of the other components undoubtedly are bioactive, exerting the overall functional benefits as an ensemble.

In summary, our study demonstrates that MSC-derived exosomes attenuate myocardial I/R injury via polarizing inflammatory macrophage towards anti-inflammatory macrophage population within the heart. miR-182 packaged in MSC-derived exosomes is involved in the modulation of macrophage polarization by targeting TLR4/NF-κB/PI3K/Akt signalling cascades.

Supplementary material

Supplementary material is available at *Cardiovascular Research* online.

Acknowledgements

We want to thank Professor Qingbo Xu for scientific advices and Dr Wei Cheng for technical assistance.

Conflict of interest: none declared.

Funding

This work was supported by the Natural Science Foundation of China (grant numbers 81470371 and 81870358); Jiangsu Provincial Key Medical Discipline

(grant number ZDXKB2016013); the Key Projects of Science and Technology of Jiangsu Province (grant number BE2016607); Jiangsu Provincial Medical Youth Talent (grant numbers QNRC2016033 and Q201610); and the Programs of the Science Foundation in Nanjing (grant numbers ZKX17011, YKK15061, and 201605015).

References

1. Hausenloy DJ, Yellon DM. Myocardial ischemia-reperfusion injury: a neglected therapeutic target. *J Clin Invest* 2013;**123**:92–100.
2. Eltzschig HK, Eckle T. Ischemia and reperfusion—from mechanism to translation. *Nat Med* 2011;**17**:1391–1401.
3. Frangogiannis NG. Regulation of the inflammatory response in cardiac repair. *Circ Res* 2012;**110**:159–173.
4. Wynn TA, Vannella KM. Macrophages in tissue repair, regeneration, and fibrosis. *Immunity* 2016;**44**:450–462.
5. Ong SB, Hernández-Reséndiz S, Crespo-Avilan GE, Mukhametshina RT, Kwek XY, Cabrera-Fuentes HA, Hausenloy DJ. Inflammation following acute myocardial infarction: multiple players, dynamic roles, and novel therapeutic opportunities. *Pharmacol Ther* 2018;**186**:73–87.
6. Golpanian S, Wolf A, Hatzistergos KE, Hare JM. Rebuilding the damaged heart: mesenchymal stem cells, cell-based therapy, and engineered heart tissue. *Physiol Rev* 2016;**96**:1127–1168.
7. Kudlik G, Hegyi B, Czibula Á, Monostori É, Buday L, Uher F. Mesenchymal stem cells promote macrophage polarization toward M2b-like cells. *Exp Cell Res* 2016;**348**:36–45.
8. Tamar BM, Radka H, Natalie LR, Tamar HA, Feinberg MS, Ihab AE, Galia B, Epstein FH, Zmira S, Smadar C. Macrophage subpopulations are essential for infarct repair with and without stem cell therapy. *J Am Coll Cardiol* 2013;**62**:1890–1901.
9. Kishore R, Khan M. More than tiny sacks: stem cell exosomes as cell-free modality for cardiac repair. *Circ Res* 2016;**118**:330–343.
10. Sluijter JP, Verhage V, Deddens JC, Van den Akker F, Doevendans PA. Microvesicles and exosomes for intracardiac communication. *Cardiovasc Res* 2014;**102**:302–311.
11. Aliotta JM, Pereira M, Wen S, Dooner MS, Del Tatto M, Papa E, Goldberg LR, Baird GL, Ventetuolo CE, Quesenberry PJ, Klinger JR. Exosomes induce and reverse monocrotaline-induced pulmonary hypertension in mice. *Cardiovasc Res* 2016;**110**:319–330.
12. Song Y, Dou H, Li X, Zhao X, Li Y, Liu D, Ji J, Liu F, Ding L, Ni Y, Hou Y. Exosomal miR-146a contributes to the enhanced therapeutic efficacy of interleukin-1β-primed mesenchymal stem cells against sepsis. *Stem Cells* 2017;**35**:1208–1221.
13. Zhang S, Chuah SJ, Lai RC, Hui J, Lim SK, Toh WS. MSC exosomes mediate cartilage repair by enhancing proliferation, attenuating apoptosis and modulating immune reactivity. *Biomaterials* 2018;**156**:16–27.
14. Xiao C, Wang K, Xu Y, Hu H, Zhang N, Wang Y, Zhong Z, Zhao J, Li Q, Zhu D. Transplanted mesenchymal stem cells reduce autophagic flux in infarcted hearts via the exosomal transfer of mir-125b. *Circ Res* 2018;**123**:564–578.
15. Mincheva-Nilsson L, Baranov V, Nagaeva O, Dehlin E. Isolation and characterization of exosomes from cultures of tissue explants and cell lines. *Curr Protoc Immunol* 2016;**115**:14.42.11–14.42.21.
16. Barile L, Cervio E, Lionetti V, Milano G, Ciullo A, Biemmi V, Bolis S, Altomare C, Matteucci M, Disilvestre D. Cardioprotection by cardiac progenitor cell-secreted exosomes: role of pregnancy-associated plasma protein-A. *Cardiovasc Res* 2018;**114**:992–1005.
17. Li G, Chen J, Zhang X, He G, Tan W, Wu H, Li R, Chen Y, Gu R, Xie J. Cardiac repair in a mouse model of acute myocardial infarction with trophoblast stem cells. *Sci Rep* 2017;**7**:44376.
18. De CG, Gallet R, Cambier L, Jaghatspanyan E, Makkar N, Dawkins JF, Berman BP, Marbán E. Exosomal microRNA transfer into macrophages mediates cellular postconditioning. *Circulation* 2017;**136**:200–214.
19. Couto GD, Liu W, Tseliou E, Sun B, Makkar N, Kanazawa H, Arditi M, Marbán E. Macrophages mediate cardioprotective cellular postconditioning in acute myocardial infarction. *J Clin Invest* 2015;**125**:3147–3162.
20. Sukma DI, Celik S, Karlsson A, Hollander Z, Lam K, Mcmanus JW, Tebbutt S, Ng R, Keown P, Mcmaster R. Exosomal miR-142-3p is increased during cardiac allograft rejection and augments vascular permeability through down-regulation of endothelial RAB11FIP2 expression. *Cardiovasc Res* 2017;**113**:440–452.
21. Wang X, Gu H, Qin D, Yang L, Huang W, Essandoh K, Wang Y, Caldwell CC, Peng T, Zingarelli B. Exosomal miR-223 contributes to mesenchymal stem cell-elicited cardioprotection in polymicrobial sepsis. *Sci Rep* 2015;**5**:13721.
22. Wu XQ, Dai Y, Yang Y, Huang C, Meng XM, Wu BM, Li J. Emerging role of microRNAs in regulating macrophage activation and polarization in immune response and inflammation. *Immunology* 2016;**148**:237–248.
23. Liu G, Abraham E. MicroRNAs in immune response and macrophage polarization. *Arterioscler Thromb Vasc Biol* 2013;**33**:170–177.
24. Shao L, Zhang Y, Lan B, Wang J, Zhang Z, Zhang L, Xiao P, Meng Q, Geng YJ, Yu XY. MiRNA-sequence indicates that mesenchymal stem cells and exosomes have similar mechanism to enhance cardiac repair. *BioMed Res Int* 2017;**2017**:4150705.
25. Xiao J, Pan Y, Li XH, Yang XY, Feng YL, Tan HH, Jiang L, Feng J, Yu XY. Cardiac progenitor cell-derived exosomes prevent cardiomyocytes apoptosis through exosomal miR-21 by targeting PDCD4. *Cell Death Dis* 2016;**7**:e2277.
26. Baglio SR, Rooijers K, Kopperslalic D, Verweij FJ, Lanzón MP, Zini N, Naaijkens B, Perut F, Niessen HWM, Baldini N. Human bone marrow- and adipose-mesenchymal stem cells secrete exosomes enriched in distinctive miRNA and tRNA species. *Stem Cell Res Ther* 2015;**6**:127.
27. Yang Y, Lv J, Jiang S, Ma Z, Wang D, Hu W, Deng C, Fan C, Di S, Sun Y, Yi W. The emerging role of Toll-like receptor 4 in myocardial inflammation. *Cell Death Dis* 2016;**7**:e2234.
28. Li C, Ha T, Kelley J, Gao X, Qiu Y, Kao RL, Browder W, Williams DL. Modulating Toll-like receptor mediated signaling by (1–>3)-beta-D-glucan rapidly induces cardioprotection. *Cardiovasc Res* 2004;**61**:538–547.
29. Vergadi E, Ieronymaki E, Lyroni K, Vaporidi K, Tsatsanis C. Akt signaling pathway in macrophage activation and M1/M2 polarization. *J Immunol* 2017;**198**:1006–1014.
30. Oyama J-I, Blais C, Liu X, Pu M, Kobzik L, Kelly RA, Bourcier T. Reduced myocardial ischemia-reperfusion injury in toll-like receptor 4-deficient mice. *Circulation* 2004;**109**:784–789.
31. Riad A, Jager S, Sobirey M, Escher F, Yaulema-Riss A, Westermann D, Karatas A, Heimesaat MM, Bereswill S, Dragun D, Pauschinger M, Schultheiss HP, Tschope C. Toll-like receptor-4 modulates survival by induction of left ventricular remodeling after myocardial infarction in mice. *J Immunol* 2008;**180**:6954–6961.
32. Timmers L, Sluijter JPG, Verlaan CWJ, Steendijk P, Cramer MJ, Emons M, Strijder C, Gründeman PF, Sze SK, Hua L, Piek JJ, Borst C, Pasterkamp G, de Kleijn DPV. Cyclooxygenase-2 inhibition increases mortality, enhances left ventricular remodeling, and impairs systolic function after myocardial infarction in the pig. *Circulation* 2007;**115**:326–332.
33. Marigo I, Dazzi F. The immunomodulatory properties of mesenchymal stem cells. *Semin Immunopathol* 2011;**33**:593–602.
34. Steinhoff G, Nesteruk J, Wolfien M, Große J, Ruch U, Vasudevan P, Müller P. Stem cells and heart disease—brake or accelerator? *Adv Drug Deliv Rev* 2017;**120**:2–24.
35. Zhang B, Yin Y, Lai RC, Tan SS, Choo ABH, Lim SK, Zhang B, Yin Y, Lai RC, Choo ABH. Mesenchymal stem cell secretes immunologically active exosomes. *Stem Cells Dev* 2014;**23**:1233–1244.
36. Ranganath SH, Levy O, Inamdar MS, Karp JM. Harnessing the mesenchymal stem cell secretome for the treatment of cardiovascular disease. *Cell Stem Cell* 2012;**10**:244–258.
37. Barile L, Lionetti V, Cervio E, Matteucci M, Gherghiceanu M, Popescu LM, Torre T, Siclari F, Moccetti T, Vassalli G. Extracellular vesicles from human cardiac progenitor cells inhibit cardiomyocyte apoptosis and improve cardiac function after myocardial infarction. *Cardiovasc Res* 2014;**103**:530–541.
38. Qin SB, Peng DY, Shi Y, Ke ZP. MiR-182-5p inhibited oxidative stress and apoptosis triggered by oxidized low-density lipoprotein via targeting toll-like receptor 4. *J Cell Physiol* 2018;**233**:6630–6637.
39. Hua F, Ha T, Ma J, Li Y, Kelley J, Gao X, Browder IW, Kao RL, Williams DL, Li C. Protection against myocardial ischemia/reperfusion injury in TLR4-deficient mice is mediated through a phosphoinositide 3-kinase-dependent mechanism. *J Immunol* 2007;**178**:7317–7324.